Higgs vacuum decay from particle collisions?

Leopoldo Cuspinera,[1,*] Ruth Gregory,[1,2,†] Katie M. Marshall,[3,‡] and Ian G. Moss[3,§]
[1]*Centre for Particle Theory, Durham University, South Road, Durham DH1 3LE, United Kingdom*
[2]*Perimeter Institute, 31 Caroline Street North, Waterloo, Ontario N2L 2Y5, Canada*
[3]*School of Mathematics, Statistics and Physics, Newcastle University, Newcastle Upon Tyne NE1 7RU, United Kingdom*

(Received 12 December 2018; published 30 January 2019)

We examine the effect of large extra dimensions on black hole seeded vacuum decay using the Randall-Sundrum model as a prototype for warped extra dimensions. We model the braneworld black hole by a tidal solution and solve the Higgs equations of motion for the instanton on the brane. Remarkably, the action of the static instanton can be shown to be the difference in the bulk areas of the seed and remnant black holes, and we estimate these areas assuming the black holes are small compared to the bulk anti–de Sitter radius. Comparing to the Hawking evaporation rate shows that small black hole seeds preferentially catalyze vacuum decay, thus extending our previous results to higher-dimensional braneworld scenarios. The parameter ranges do not allow for standard model Higgs decay from collider black holes, but they can be relevant for cosmic ray collisions.

DOI: 10.1103/PhysRevD.99.024046

I. INTRODUCTION

A fascinating consequence of the discovery of the Higgs [1,2] is that the standard model vacuum appears to be metastable [3–7] (see also earlier work [8–12]). Although it was originally thought that this would not be an issue due to the extremely long half-life predicted by the classic bubble nucleation arguments of Coleman *et al.* [13–15] (see also [16]), recent work by two of us [17–21] indicates that the situation may not be quite so rosy. In [17], we developed a description of vacuum decay catalyzed by black holes, with the result that the strong local spacetime curvature of small black holes catalyzes vacuum decay and dramatically changes the prediction for the lifetime of the universe.[1] Tunneling is initiated by a black hole seed in the false vacuum that decays into a remnant black hole surrounded by Higgs fields that have overcome the potential barrier and lie in a lower energy state. The tunneling rate is determined by the difference in action between the remnant black hole–instanton combination and the seed black hole false vacuum configuration that turns out to be proportional to the difference in the horizon area of the seed and remnant black holes. Because of this dependence on the black hole area, enhancement occurs only for very small black holes, the obvious candidates being primordial black holes in our universe; indeed, there is an interesting thermal interpretation of our result (see, for example, [23–25]).

There is, however, another possible scenario in which small black holes could occur, and that is in particle collisions. If we have a situation where our four-dimensional Planck scale is derived from a higher-dimensional Planck mass close to the standard model scale [26–29], then it is easier to form black holes in particle collisions [30–33]. Such higher-dimensional theories are dubbed *large extra dimension* scenarios, and the premise is that we live on a four-dimensional "brane" in a higher-dimensional spacetime. Our relatively high Planck scale, $M_p = 1/\sqrt{8\pi G_N}$, is the result of a geometric hierarchy coming from an integration over the extra dimensions. Since the true Planck scale is the higher-dimensional one, it is easier to form black holes in high energy processes, leading to the possibility of black holes being produced at the LHC (for a review see [34]). Given this exciting possibility for producing small black holes, we should revisit our four-dimensional black hole instanton calculations and explore the impact of large extra dimensions.

As a first step in looking at vacuum decay with extra dimensions, we considered the impact of dimensionality on our toy model thin wall calculations in [19], finding that extra dimensions seemed to impede vacuum decay; however, these estimates were predicated on a rather crude higher-dimensional generalization that did not take the

*j.l.cuspinera@durham.ac.uk
†r.a.w.gregory@durham.ac.uk
‡k.marshall6@newcastle.ac.uk
§ian.moss@newcastle.ac.uk

[1]Some of these results were examined in [22], however, without explicitly computing the Euclidean instanton action.

braneworld aspect of the large extra dimension models into account. In this paper, we revisit the role of large extra dimensions in vacuum decay, explicitly modeling the brane black hole and finding exact solutions for the instanton on the brane. We also make a more careful estimation of the black hole Hawking radiation rate on the brane. We find that, while for a given seed mass the higher-dimensional tunneling rate is indeed lower than the four-dimensional one, what we gain from higher dimensions is that lower seed masses are allowed due to the lower value of the fundamental Planck scale, M_D.

The layout of the paper is as follows: in the next section, we review the status of constructing instantons both in four dimensions with black holes and for braneworlds in five dimensions without black holes, and discuss the problems involved in introducing a black hole to the higher-dimensional calculation. In Sec. III we discuss the calculation of the action of an approximate black hole instanton, showing that, as in four dimensions, the static instanton action is the difference in black hole horizon areas. In Sec. IV we solve for the brane scalar field and find the instantons and their actions numerically. In Sec. V we conclude.

II. BRANEWORLDS AND BLACK HOLES

It is perhaps worth recalling the various challenges in finding an instanton for vacuum decay in a braneworld setting. The braneworld paradigm describes our universe as an effective submanifold of a higher-dimensional manifold, with standard model fields living only on the four-dimensional braneworld, but with gravity propagating throughout all of the dimensions, leading to the renormalization of Newton's constant. For one extra dimension we can consistently solve for the spacetime geometry using the Israel approach [35], giving the standard Randall-Sundrum (RS) braneworld [29], a paradigm for warped compactifications. For higher codimension, there is no unique "delta-function" limit for a thin braneworld [36], and typically one resorts to approximate hybrid Kaluza-Klein/warped descriptions for gravity on a lower-dimensional brane. Thus, for a concrete gravitational description in this paper we will remain within the RS model.

The RS model supposes that we have one extra dimension, and that the higher-dimensional spacetime, or bulk, has a negative cosmological constant. The braneworld has a positive tension, and the vacuum brane has an energy-momentum tensor that is parallel to the brane with energy and tension equal. The original solution presented by Randall and Sundrum had the tension tuned to give a flat brane:

$$ds^2 = e^{-2|z|/\ell}\eta_{\mu\nu}dx^\mu dx^\nu - dz^2, \tag{1}$$

where the cusp in the warp factor at $z = 0$ corresponds to the brane. The local negative curvature of the bulk supports the brane tension σ that is easily calculated from the Israel junction conditions,

$$\mathcal{K}^{(+)}_{\mu\nu} = -\frac{1}{\ell}\eta_{\mu\nu} \Rightarrow 8\pi G_5\sigma\eta_{\mu\nu} = \Delta\mathcal{K}_{\mu\nu} - \Delta\mathcal{K}\eta_{\mu\nu} = \frac{6}{\ell}\eta_{\mu\nu}, \tag{2}$$

and is tuned to fit with the cosmological constant $\Lambda_5 = -6/\ell^2$. Detuned branes, with tension greater or less than this critical value may also be embedded within the bulk anti–de Sitter (AdS) spacetime, although the natural embeddings now become either spacelike or timelike [37–42], but as long as the brane energy momentum is approximately homogeneous (i.e., having a spatially isotropic pressure term only), the bulk solution can be fully integrated, and the brane trajectory found [41].

For a brane black hole solution, we must break this spatial homogeneity, but even with the added benefit of having only one codimension, the exact solution for a brane black hole has been extremely elusive [43,44]. The natural geometry of a Schwarzschild black hole that extends off the brane into a black string, found by Chamblin, Hawking, and Reall [45], has the problem that it is neither representative of matter localized on the brane nor stable, suffering from a Gregory-Laflamme type of instability [46,47]. A lower-dimensional analogue of the brane black hole was found by Emparan *et al.* [48,49] by taking a $(2+1)$-dimensional brane through the equatorial plane of a four-dimensional AdS C-metric [50,51]. The black hole would be expected to be accelerating from the perspective of the bulk, since an observer hovering at a fixed distance from the brane is, in fact, undergoing uniform acceleration toward it. Unfortunately, there is no known exact solution for a C-metric in more than four dimensions, and thus no template for constructing a braneworld black hole plus bulk analytically.

To maintain an analytic approach one can explore the effective brane gravitational equations using the approach of Shiromizu *et al.* [52], leading to the tidal solution that we will use in this paper [53]. (One can also explore braneworlds with additional matter, either on the brane or in the bulk, to support analyticity of the brane embedding; see, e.g., [54–57].) Alternately, one can take a numerical approach; the equations of motion to be solved are an elliptic system [58], with the brane junction conditions and asymptotic Poincarè horizon providing the boundary conditions. The solutions for small black holes were found in [59], although the large black hole solutions have been far trickier to determine due to the nonlinearity of the Einstein equations and the impact of the bulk warping of the horizon; however, there has been some interesting recent work in this direction [60,61].

Now let us consider the instanton from a higher-dimensional perspective. The decay of a metastable false vacuum was first computed by Coleman and collaborators in a series of papers [13–15] in which a Euclidean approach was used to find an instanton solution interpolating between the true and false vacua. A convenient approximation, extremely useful for visualization, is to take the region over which the vacuum interpolates to be very narrow

in comparison with the interior of the bubble. This "thin wall" then has a straightforward generalization to gravity, as described in the paper with de Luccia [15] (CDL). While this thin wall description is not appropriate for the Higgs vacuum decay [20], where the vacuum interpolation is very wide and relatively gentle, it nonetheless provides an excellent shorthand for visualizing the process of decay.

The CDL picture, however, is very symmetric and assumes that both the initial and the final states are completely devoid of features and are homogeneous. If instead one relaxes this assumption, minimally, by allowing for an inhomogeneity in the form of a black hole, the analytic approach of CDL can be preserved, and the equations of motion for the instanton are only minimally altered [17–20]; however, the impact on the action of the instanton can be quite significant, and particularly for the thick scalar domain walls appropriate to the Higgs potential [20], tunneling turns out to be significantly enhanced to the extent that if there are primordial black holes, false vacuum decay will happen.

Let us now consider how these arguments might lift to higher dimensions. In [62], the equivalent of the CDL instantons on a Randall-Sundrum braneworld were constructed, the five-dimensional (5D) instanton being geometrically akin to the four-dimensional (4D) representations of the CDL instantons. Sub- and supercritical branes follow spherical trajectories in the AdS bulk, so the tunneling of a Minkowski false vacuum to an AdS true vacuum is represented by a flat brane with a bubble sticking out, as shown in Fig. 1. As is usual with the RS model, two copies of the picture are identified, and the "bubble wall" is the sharp edge between the spherical and flat parts of the braneworld, appearing roughly as a codimension two object.

Ideally, one would like to construct a similar instanton, but with a black hole; however, at this point the lack of an exact brane black hole solution becomes problematic. Even if we drop a dimension to have a $(2+1)$-dimensional braneworld, for which the brane black hole solution is constructed via the C-metric [48], we have the problem that the C-metric has a unique slicing for the braneworld [63], so we cannot patch together two different braneworld trajectories such as an equatorial subcritical slice matching to a flat brane further away as suggested in Fig. 2. Indeed, slicing a bulk Schwarzschild metric induces additional energy momentum on the brane [54,55] (except for the uniform radius "cosmological" brane solutions).

Thus as a direct approach to finding the instanton seems problematic, we follow a more pragmatic approach, and rather than seeking an exact analytic solution, instead consider what a black hole instanton might approximately look like. From the intuition gleaned in the 4D black hole instantons, we expect that small black holes are the most dangerous, and that the dominant instanton will be the static instanton [20]. Then, analogous to the modeling of collider black hole phenomenology [64], we use the higher-dimensional Schwarzschild-AdS solution as an approximation to the local bulk black hole: this allows us to construct a method of calculating the instanton action formally. Finally, in order to correctly identify the asymptotics of our instanton, we need a way of interpolating between the near horizon and far-field brane solution, which we expect to have a 4D Schwarzschild $G_N M/r$ behavior. This final step requires a choice for the braneworld solution, and we use the tidal brane solution of Dadhich *et al.* [53], found by considering vacuum solutions with a nonvanishing bulk Weyl tensor in the formalism of Shiromizu *et al.* [52]. The tidal solution has the attractive feature that it has the correct asymptotic form at a large brane radius, but it looks like the five-dimensional Schwarzschild potential for a small radius; indeed, it is similar to the Reissner-Nordstrom black hole, although the "tidal charge" term $-r_Q^2/r^2$ is negative. This tidal charge was not related to the mass in [53], but left as an arbitrary degree of freedom. Therefore, part of our task in Sec. IV will be to relate the tidal charge to the mass of the black hole.

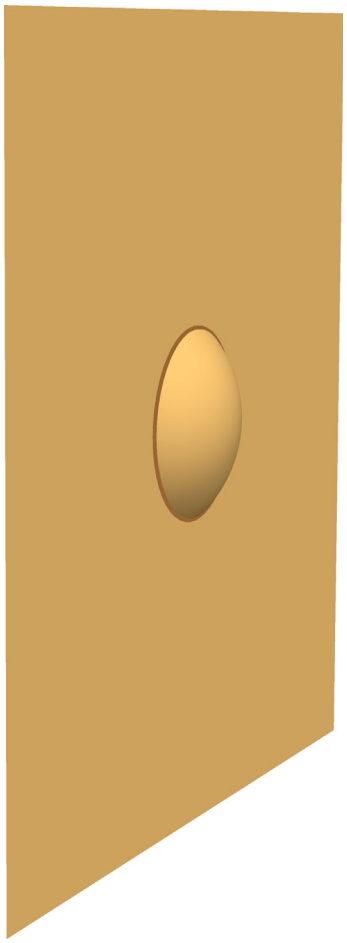

FIG. 1. The braneworld instanton for decay of a Minkowski false vacuum brane to a subcritical AdS brane from [62].

Our strategy is then as follows: we first take our brane black hole, approximately modeled by the 5D

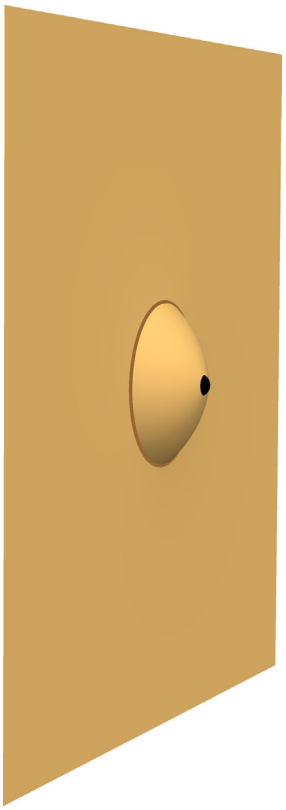

FIG. 2. The expected geometry of braneworld vacuum decay with a braneworld black hole.

Schwarzschild-Ads solution, and continue to Euclidean time. We then compute the action of this solution in a rather general way, using the approach of Hawking and Horowitz [65]; as per usual, the direct way of computing the action leads to an apparent divergence that we cannot in this case regulate directly by introducing a cutoff as we will explain. Nonetheless, however, we choose to regulate the action, and the same method will apply for the false vacuum black hole and the instanton bubble solution. Thus we simply subtract the seed and bubble actions to get the final amplitude for vacuum decay. Crucially, this turns out to be simply the difference in areas of the seed and remnant black hole horizon geometries. Finally, we integrate the scalar equations of motion on the brane to obtain the brane bubble solution, and we use the tidal metric to relate the near horizon and asymptotic geometries. The net result is an amplitude for brane black hole seeded vacuum decay that we can compare to the higher-dimensional brane black hole evaporation rate to explore whether brane vacuum metastability is an issue.

III. THE EUCLIDEAN BRANE BLACK HOLE ACTION

In this section we will show that, just as in four dimensions, the Euclidean action of any static black hole solution can be expressed entirely by surface terms. This is a remarkable result, because it not only applies to the vacuum black hole, it also applies with a cosmological constant, with matter and even with a conical singularity at the horizon.

We begin by recalling the properties of the Euclidean Schwarzschild black hole in four dimensions,

$$ds^2 = f(r)d\tau^2 + f(r)^{-1}dr^2 + r^2 d\Omega_{II}^2, \tag{3}$$

where

$$f(r) = 1 - \frac{2G_N M}{r}. \tag{4}$$

In order to explore the geometry near the "horizon" $r_h = 2G_N M$, we expand using a new coordinate ϱ, defined by

$$\varrho = \sqrt{\frac{2(r - r_h)}{\kappa}}, \tag{5}$$

where κ is the surface gravity, $\kappa = f'(r_h)/2$. To leading order $f(r) = \kappa^2\varrho^2 + O(\varrho^4)$, and close to the horizon,

$$ds^2 = d\varrho^2 + \varrho^2 d(\kappa\tau)^2 + r_h^2 d\Omega_{II}^2 + O(\varrho^4), \tag{6}$$

For small $\varrho \geq 0$, the metric is geometrically the product of a disk with a sphere, provided that $\kappa\tau$ is taken to be an angular coordinate with the usual range 2π. If $\kappa\tau$ has a different range, then the manifold has a conical singularity at r_h. Note that the Euclidean section is perfectly regular other than this, but only covers the exterior region of the original black hole. The *event* horizon of the original Lorentzian black hole is encoded in the topology of the Euclidean solution: the surface $\varrho = 0$ is a 2-sphere of radius r_h.

For the brane black hole in five dimensions, the metric is extended into an additional direction, parametrized by χ in Kudoh *et al.* [59], who numerically constructed small brane black holes with the horizon size less than the AdS radius ℓ. In [59], the metric was written in the form

$$ds^2 = \frac{1}{(1 + \frac{\rho}{\ell}\cos\chi)^2}[T^2(\rho,\chi)d\tau^2 + e^{2B(\rho,\chi)}(d\rho^2 + \rho^2 d\chi^2) + e^{2C(\rho,\chi)}\rho^2 \sin^2\chi d\Omega_{II}^2], \tag{7}$$

where the brane sits at $\chi = \pi/2$, and $\chi \leq \pi/2$ is kept as the bulk. Clearly, in the small black hole limit, $\ell \to \infty$, we have the five-dimensional Schwarzschild black hole,

$$ds^2 = \left(\frac{\rho^2 - \rho_h^2}{\rho^2 + \rho_h^2}\right)^2 d\tau^2 + \left(\frac{\rho^2 + \rho_h^2}{\rho^2}\right)^2 [d\rho^2 + \rho^2 d\Omega_{III}^2], \tag{8}$$

written here in homogeneous coordinates, rather than the area gauge. The local Euclidean horizon coordinate is $\varrho = 2(\rho - \rho_h)$, and the horizon has area $\mathcal{A} = 4\rho_h^2$ and surface gravity

$$\kappa = e^{-B(\rho_h)} T'. \tag{9}$$

The black hole is corrected at order ρ/ℓ by the conformal factor, and at order ρ_h/ℓ in the other metric functions close to the horizon. Kudoh and collaborators integrated the functions T, B, and C numerically and found that the T function to a very good approximation extends hyperspherically off the brane. Although B and C are not precisely the same, their difference is roughly of order ρ_h/ℓ as expected. At large ρ, $T, B, C \to 1$, and the metric is asymptotically AdS in the Poincaré patch.

We do not use the explicit form of the metric; however, the features we require from the solutions of [59] are that the event horizon is topologically hyperspherical with constant surface gravity, and that the braneworld black hole asymptotes the Poincaré patch of AdS. The coordinate transformation between the local black hole coordinates and the Poincaré RS coordinates is

$$\rho^2 = r^2 + \ell^2 (e^{|z|/\ell} - 1)^2, \quad \tan\chi = \frac{r}{\ell(e^{|z|/\ell} - 1)}, \tag{10}$$

and we expect that the "trajectory" of the brane in the black hole metric will bend slightly in response to the black hole at ρ_h, giving rise to a four-dimensional Newtonian potential as described in [66]. From the perspective of the $\{\rho, \chi\}$ coordinates, in which the brane sits at $\chi = \pi/2$, this will show up as a $1/\rho$ correction to T, B, C. We therefore take our asymptotic metric to be of the form

$$ds^2 = e^{-2|z|/\ell}[F(r,z)d\tau^2 + F(r,z)^{-1}dr^2 + r^2 d\Omega^2] + dz^2, \tag{11}$$

where $F \sim 1\text{–}2G_N M(z)/r + O(r^{-2})$. We can think of $M(z)$ as coming from the brane bending term of M/ρ in the original coordinates.

A. Computing the action

The action of the black hole instanton combination diverges and has to be regulated in some way. We do this by truncating the five-dimensional manifold at large distances from the black hole, taking a surface at large radius R on the brane, and extending this along geodesics in the $\pm z$ directions orthogonal to the brane to produce the outer boundary surface $\partial\mathcal{M}_R$ as indicated in the cartoon in Fig. 3. The interior is denoted by $\mathcal{M}_R$, and the intersection of $\mathcal{M}_R$ with the braneworld is denoted by $\mathcal{B}$.

The Euclidean action for this truncated instanton or black hole solution is

$$I_R = -\frac{1}{16\pi G_5}\int_{\mathcal{M}_R}(R_5 - 2\Lambda_5)\sqrt{g_5} + \int_{\mathcal{B}}\mathcal{L}_m\sqrt{g_4} + \frac{1}{8\pi G_5}\int_{\partial\mathcal{M}_R} K\sqrt{h}, \tag{12}$$

where K denotes the extrinsic curvature of the boundary surface $\partial\mathcal{M}_R$ defined with an *inward* pointing normal to the bulk manifold $\mathcal{M}_R$. The matter Lagrangian $\mathcal{L}_m$ includes the contribution from any nontrivial Higgs field profile, as well as the brane stress-energy tensor. The bulk integral is understood to range across all z and includes the δ-function curvature at the brane source in the spirit of the Israel approach. Numerical subscripts distinguish between bulk and brane geometry, with the gravitational constant in five dimensions given in terms of Newton's constant G_N by $G_5 = \ell G_N$.

We now show that the tunneling exponent, given by the difference between the actions of the instanton geometry with a remnant black hole and the false vacuum geometry with the seed black hole: $B = I_{\rm inst} - I_{\rm FV}$ is finite in the limit $R \to \infty$. The first step is to introduce a small ball, $\mathcal{H}$,

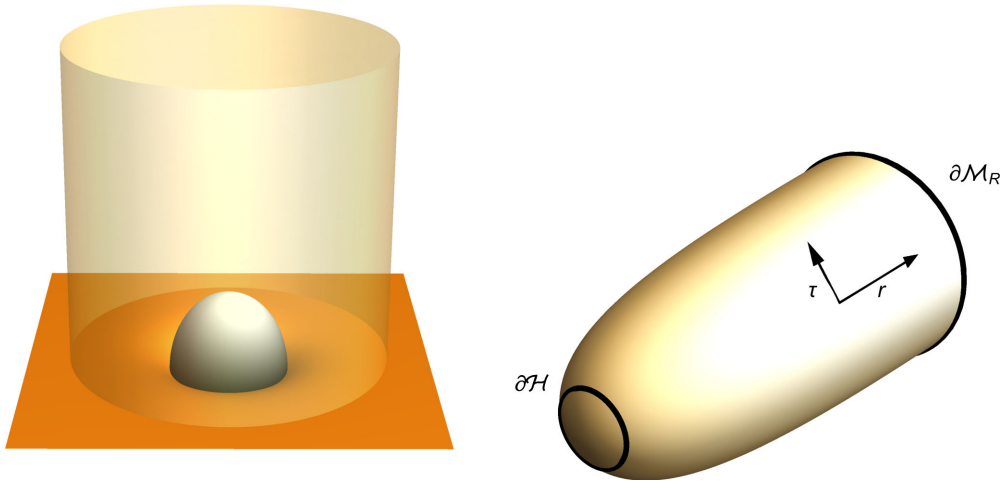

FIG. 3. A cartoon of the Euclidean tidal black hole and the cutoff surfaces. On the left, the τ, θ coordinates are suppressed, and the cutoff surface is indicated relative to the brane and bulk black hole horizon. Only one-half of the $\mathbb{Z}_2$ symmetric solution is shown. On the right, the Euclidean τ coordinate is shown, but the bulk and angular coordinates are suppressed, and the "black hole cigar" geometry is indicated. Two circles denote the boundary $\partial\mathcal{H}$ of the region just outside the horizon and the boundary $\partial\mathcal{M}_r$ at large radius.

extending a proper distance of order $\mathcal{O}(\varepsilon)$ out from the black hole event horizon, to formally deal with any conical deficits arising from a generic periodicity in Euclidean time. This splits the action calculation into two terms,

$$I_R = I_R^{\rm hor} + I_R^{\rm ext}, \tag{13}$$

where[2]

$$I_R^{\rm hor} = -\frac{1}{16\pi G_5}\int_{\mathcal{H}}(R_5 - 2\Lambda_5)\sqrt{g_5} + \int_{\mathcal{B}_{\mathcal{H}}}\mathcal{L}_m\sqrt{g_4} + \frac{1}{8\pi G_5}\int_{\partial\mathcal{H}} K\sqrt{h}, \tag{14}$$

$$I_R^{\rm ext} = -\frac{1}{16\pi G_5}\int_{\mathcal{M}_R-\mathcal{H}}(R_5 - 2\Lambda_5)\sqrt{g_5} + \int_{\mathcal{B}-\mathcal{B}_{\mathcal{H}}}\mathcal{L}_m\sqrt{g_4} + \frac{1}{8\pi G_5}\int_{\partial\mathcal{H}} K\sqrt{h} + \frac{1}{8\pi G_5}\int_{\partial\mathcal{M}_R} K\sqrt{h}, \tag{15}$$

and $\mathcal{B}_{\mathcal{H}} = \mathcal{B}\cap\mathcal{H}$ is the intersection of the event horizon cap with the brane.

In order to deal with the near-horizon contribution, we transform (7) to local horizon coordinates, analogous to the Euclidean Schwarzschild transformation, Eq. (5), so that

$$ds^2 \approx d\varrho^2 + A^2(\varrho,\xi)d\tau^2 + D^2(\varrho,\xi)d\Omega_{II}^2 + N^2(\varrho,\xi)d\xi^2, \tag{16}$$

where $\varrho < \varepsilon$ inside $\mathcal{H}$. Comparing to (7), we see $A = T/(1+\frac{\rho}{\ell}\cos\chi)$, $D = \rho\sin\chi e^C/(1+\frac{\rho}{\ell}\cos\chi)$, with $\varrho \approx (\rho-\rho_h)/(1+\frac{\rho_h}{\ell}\cos\chi)$ and $\xi = \chi + \mathcal{O}(\varrho^2)$. The brane sits at $\xi = \pi/2$, and on the horizon, $\xi\in[0,\pi]$.

As with the four-dimensional Euclidean Schwarzschild, there is a natural periodicity of τ for which the Euclidean metric is nonsingular; this periodicity is $\beta_0 = 2\pi/\kappa$, where κ is the surface gravity of the black hole given in the original coordinates by (9), and in the horizon coordinates by $\partial A/\partial\varrho$. From nonsingularity of the geometry, we deduce $N\sim N_0(\xi)+\mathcal{O}(\varrho^2)$, $D\sim D_0(\xi)+\mathcal{O}(\varrho^2)$, and $A\sim\kappa\varrho+\mathcal{O}(\varrho^2)$. Now let us consider a general periodicity β for the Euclidean time τ, and then we will have a conical singularity at $\varrho=0$. In order to compute the action, we smooth this out by modifying the A function so that $A'(\varepsilon,\xi)=\kappa$, but $A'(0,\xi)=\kappa\beta_0/\beta$. Computing the curvature for this smoothed metric gives

$$\sqrt{g_5}(R_5 - 2\Lambda_5) = -2N_0(\xi)D_0(\xi)^2A''(\varrho) + \mathcal{O}(\varrho), \tag{17}$$

which gives the bulk contribution to $I_R^{\rm hor}$ as

$$\begin{aligned} &-\frac{1}{16\pi G_5}\int_{\mathcal{H}}(R_5-2\Lambda_5)\sqrt{g_5} + \int_{\mathcal{B}_{\mathcal{H}}}\mathcal{L}_m\sqrt{g_4} \\ &= \frac{\beta}{2G_5}[A'(\varepsilon)-A'(0)]\int N_0D_0^2d\xi + \mathcal{O}(\varepsilon^2) \\ &= \frac{\kappa}{8\pi G_5}[\beta-\beta_0]\mathcal{A}_5, \end{aligned} \tag{18}$$

where $\mathcal{A}_5 = 4\pi\int N_0D_0^2d\xi$ is the area of the braneworld black hole horizon extending into the bulk (on both sides of the brane). Note that the matter term on the left gives no contribution since the matter Lagrangian does not have a singularity at $\rho=0$.

To compute the Gibbons-Hawking boundary term we note that the normal to $\partial\mathcal{H}$ is $n=-d\varrho$; hence the extrinsic curvature is

$$K = -A^{-1}A_{,\varrho} + \mathcal{O}(\varepsilon) \tag{19}$$

and

$$\frac{1}{8\pi G_5}\int_{\partial\mathcal{H}} K\sqrt{h} = -\frac{\kappa\beta}{2G_5}\int N_0D_0^2d\xi = -\frac{\kappa\beta\mathcal{A}_5}{8\pi G_5}. \tag{20}$$

Thus the contribution to the action from the horizon region is

$$I_R^{\rm hor} = -\frac{\kappa\beta_0\mathcal{A}_5}{8\pi G_5} = -\frac{\mathcal{A}_5}{4G_5}. \tag{21}$$

In Appendix A, we show that the external part $I_R^{\rm ext}$ can be simplified by taking a canonical decomposition based on a foliation of the manifold by surfaces of constant τ, Σ_τ, and the part of the action outside the horizon cylinder reduces to simple surface terms,

$$I_R^{\rm ext} = \frac{1}{8\pi G_5}\int_0^\beta d\tau\left(\int_{C_R}{}^3K\sqrt{h} + \int_{C_{\mathcal{H}}}{}^3K\sqrt{h}\right), \tag{22}$$

where ${}^3K$ are the extrinsic curvatures of codimension two surfaces of constant r, regarded as submanifolds of surfaces of constant τ, Σ_τ, as described in Appendix A.

Close to the horizon, we use the metric (16) and find

$${}^3K = 2D^{-1}D_{,\varrho} + N^{-1}N_{,\varrho} \to 0, \tag{23}$$

at the horizon $\varrho=0$ for the behavior of the metric coefficients $D(\varrho,\xi)$ and $N(\varrho,\xi)$ given earlier. There is no contribution to the action from this boundary term.

At large distances, the metric approaches the perturbed Poincaré form (11), and we find

$${}^3K = -\frac{2}{R}e^{|z|/\ell}F^{1/2}, \qquad \sqrt{h} = R^2e^{-3|z|/\ell}F^{1/2}; \tag{24}$$

hence

[2]Note, the extrinsic curvature in the Gibbons-Hawking term is computed with an inward pointing normal, hence the *same* sign for that term in each expression.

$$I_R^{\rm ext} = -\frac{\beta}{G_N \ell}\int_0^\infty dz e^{-2z/\ell}(2R - 4G_N M(z) + O(R^{-1})). \tag{25}$$

Ideally, we would like to regularize this action either by background subtraction or by adding in boundary counterterms along the lines of [67,68]; however, the counterterms of [68] do not regulate this action, and one cannot replace the interior of $\mathcal{M}_R$ with a pure RS braneworld, due to the variation of $M(z)$ along $\partial\mathcal{M}_R$. Instead, we note that the Higgs fields on the brane in any instanton solution will die off exponentially for large r, so from the intuition that $M(z)/r \sim M_\infty/\rho = M_\infty/\sqrt{r^2 + \ell^2(e^{|z|/\ell} - 1)^2}$, we then deduce that the mass function $M(z)$ will be the same at leading order for both the false vacuum with the seed brane black hole and the instanton solution. Therefore, the exterior terms will cancel when we take the difference between the instanton action and the false vacuum action,

$$B = I_{\rm inst} - I_{\rm FV} = \lim_{R\to\infty}[I_R^{\rm ext}|_{\rm inst} - I_R^{\rm ext}|_{\rm FV}] - \frac{\mathcal{A}_5^{\rm inst}}{4G_5} + \frac{\mathcal{A}_5^{\rm FV}}{4G_5} = \frac{\mathcal{A}_S}{4G_5} - \frac{\mathcal{A}_R}{4G_5}, \tag{26}$$

where $\mathcal{A}_S$ and $\mathcal{A}_R$ refer to the areas of the seed and remnant black hole horizon areas, respectively.

This is simply the reduction in entropy $-\Delta S$ caused by the decay process, and the tunneling rate is recognizable as the probability of an entropy reduction $\propto \exp(\Delta S)$. The difficulty we face when applying (26) is that we have to relate the black hole area to the mass of the black hole triggering the vacuum decay and the physical parameters in the Higgs potential. This requires explicit solutions for the gravitational and Higgs fields.

IV. TIDAL BLACK HOLE BUBBLES

As we reviewed, the main obstacle to finding tunneling instantons is the lack of any analytic brane black hole solutions. The brane-vacuum equations are complicated by the reduced symmetry of the expected static, brane-rotationally symmetric geometry. Although we have numerical brane black hole solutions, once we introduce Higgs profiles on the brane, these would be modified, and a new full numerical brane + bulk solution would have to be computed—a formidable task. Instead, we adopt a more practical alternative, based on the tidal black hole solutions of Dadhich *et al.* [53].

As described, for example, by Maartens [69], one can take an approach of solving purely the brane "Einstein equations," i.e., the induced Einstein equations on the brane found by the Gauss Codazzi projection of the Einstein tensor in Shiromizu *et al.* [52] (SMS). These equations are similar to the four-dimensional Einstein equations, but contain additional terms involving the square of the energy momentum of any matter on the brane, and an additional so-called Weyl tensor, $\mathcal{E}_{\mu\nu}$, coming from a projection of the bulk Weyl tensor onto the brane. The Weyl tensor for the tidal black hole satisfies the equations $\mathcal{E}_\mu{}^\mu = 0$ and $\nabla^\mu\mathcal{E}_{\mu\nu} = 0$. Following [69], one uses the symmetry of the physical setup to write the Weyl tensor as

$$\mathcal{E}^\mu_\nu = \mathrm{diag}\left(\mathcal{U}, -\frac{(\mathcal{U}+2\Pi)}{3}, \frac{\Pi-\mathcal{U}}{3}\right). \tag{27}$$

This is manifestly trace-free, and the "Bianchi" identity implies a conservation equation for $\mathcal{U}$, Π. For the spherically symmetric static brane metric

$$ds^2_{\rm brane} = f(r)e^{2\delta(r)}d\tau^2 + f^{-1}(r)dr^2 + r^2 d\Omega_{II}^2, \tag{28}$$

the conservation equation implies

$$(\mathcal{U}+2\Pi)' + \left(\frac{f'}{f} + 2\delta'\right)(2\mathcal{U}+\Pi) + \frac{6\Pi}{r} = 0. \tag{29}$$

Even for the vacuum brane this is not a closed system, but if one assumes an equation of state, one can find an induced brane solution [70]. The tidal black hole corresponds to the choice $\Pi = -2\mathcal{U}$, for which (29) is easily solved by $\mathcal{U} \propto 1/r^4$.

The tidal black hole of Dadhich *et al.* [53] has $\delta(r) \equiv 0$,

$$f(r) = 1 - \frac{2G_N M}{r} - \frac{r_Q^2}{r^2}, \tag{30}$$

and

$$\mathcal{E}_{\mu\nu}dx^\mu dx^\nu = -\frac{r_Q^2}{r^4}(f(r)d\tau^2 + f^{-1}(r)dr^2 - r^2 d\Omega^2), \tag{31}$$

where r_Q is a constant parameter related to the tidal charge Q of [53] by $r_Q^2 = -Q$. The motivation for this solution is clear: at large distances, the Newtonian potential of a mass source has the conventional $G_N M/r$ behavior due to a "brane-bending" term identified by Garriga and Tanaka [66]; the interpretation being that the brane shifts relative to the bulk in response to matter on the brane. At small distances, on the other hand, we would expect the higher-dimensional Schwarzschild potential to be more appropriate, hence the $-r_Q^2/r^2$ term. The event horizon is distorted by the Weyl tensor, hence the name. Other choices for the Weyl tensor lead to different brane solutions [70]; however, these tend to have either wormholes or singularities (or both). Therefore, we do not consider these here.

For our bubble solution, we will need to find the fully coupled Higgs plus brane SMS-gravitational equations of motion in the spherically symmetric gauge (28), and we will use the same *tidal* Ansatz for the equation of state of the Weyl tensor: $\Pi = -2\mathcal{U}$. The beauty of the tidal Ansatz is that even with the Higgs fields taking a nontrivial bubble

profile, the conservation equation for the Weyl tensor (29) is still solved by $\mathcal{U} = -r_Q^2/r^4$.

We also have some limited information about the form of the tidal black hole solution away from the brane from an expansion in the fifth coordinate. According to Maartens and Koyama [71], the metric parallel to the brane at proper distance z from the brane is

$$\tilde{g}_{\mu\nu}(z) = g_{\mu\nu}(0) - (8\pi G_5 S_{\mu\nu})z + [(4\pi G_5)^2 S_{\mu\sigma}S^{\sigma}{}_{\nu} - 8\pi G_N S_{\mu\nu} - \mathcal{E}_{\mu\nu}]z^2 + \cdots, \tag{32}$$

where $S_{\mu\nu} = T_{\mu\nu} - \frac{1}{3}T g_{\mu\nu}$ is composed of the energy momentum tensor of brane matter. In the false vacuum state, we have $T_{\mu\nu} = 0$, and the metric expansion away from the brane reduces to

$$\begin{aligned} ds^2 &\approx e^{-2|z|/\ell}(g_{\mu\nu} - \mathcal{E}_{\mu\nu}z^2) + dz^2 \\ &\approx e^{-2|z|/\ell}\left\{\left(1 + \frac{r_Q^2 z^2}{r^4}\right)(f d\tau^2 + f^{-1}dr^2) \right. \\ &\quad \left. + \left(1 - \frac{r_Q^2 z^2}{r^4}\right) r^2 d\Omega_{II}^2\right\} + dz^2, \end{aligned} \tag{33}$$

which clearly shows how the horizon area decreases in the z direction. The horizon forms into a true bulk black hole when the area vanishes for some value of z of order r_h^2/r_Q.

Although this tidal black hole has many attractive features, the main difficulty that has to be overcome when finding the bubble solutions is that the tidal constant r_Q is undetermined. Clearly a nonsingular brane black hole, if approximately tidal, should have a relation between the asymptotic mass measured on the brane, M, and the tidal charge r_Q^2. For very large black holes, we expect the horizon radius to be predominantly determined by M, and this ambiguity is not relevant; however, for the small black holes we are interested in, the horizon radius is primarily dependent on r_Q, and we must confront this ambiguity.

We start by noting that the tidal black hole solution should be identical to the five-dimensional Schwarzschild black hole in the limit that the AdS radius $\ell \to \infty$, as the brane stress-energy tensor, which is tuned to the cosmological constant, vanishes in this limit, and full $SO(4)$ rotational symmetry is restored. Since $G_N = G_5/\ell$, Eq. (30) implies that $r_Q^2 \to r_h^2$ in this limit. Intuitively, we also expect that for small black holes, the bulk AdS scale should also be subdominant, and the black hole should look (near the horizon at least) mainly like a five-dimensional black hole, i.e., $r_Q^2 \to r_h^2$ as $r_h \to 0$. We will therefore assume analyticity in r_h/ℓ and write

$$r_Q^2 = r_h^2\left(1 - b\frac{r_h}{\ell} + \mathcal{O}\left(\frac{r_h^2}{\ell^2}\right)\right) \tag{34}$$

for small r_h/ℓ, where b is some constant independent of r_h and ℓ, expected to be roughly of order unity. For the tidal black hole, a trivial rewriting of (30) gives the relation

$$M = \frac{b r_h^2}{2G_5}. \tag{35}$$

In other words, we have expressed the ambiguity in the tidal parameter for small black holes by the parameter b, and the relationship between the asymptotic mass of the black hole as measured on the brane and the horizon radius explicitly factors in this ambiguity. As we now see, this uncertainty can be absorbed into a redefinition of the low energy Planck scale in the tunneling rate.

The tunneling process starts with the uniform false vacuum ϕ_v and a seed black hole with mass M_S. This false vacuum configuration resembles the tidal black hole on the brane, and a slightly perturbed 5D Schwarzschild solution in the bulk [59]. The bubble solution represents the decay process to another state with the field asymptoting the same false vacuum at large distances but with the field approaching its true vacuum near the horizon of a remnant black hole with mass M_R, which remains after tunneling.

In the previous section we showed that the tunneling exponent is given by

$$B = \frac{1}{4G_5}(\mathcal{A}_S - \mathcal{A}_R), \tag{36}$$

where S represents the seed black hole area and R that of the remnant black hole (recall, this area is the full five-dimensional area of the horizon extending into the bulk). To leading order in r_h/ℓ, the small black hole horizon has an approximately hyperspherical shape, therefore the area will be well approximated by $2\pi^2 r^3$, and hence

$$B = \frac{\pi^2}{2G_5}(r_S^3 - r_R^3) = \frac{\pi^2 r_S^3}{2G_5}\left[1 - \left(\frac{M_R}{M_S}\right)^{\frac{3}{2}}\right] \tag{37}$$

using (35). In the limit that the difference in seed and remnant black hole masses is small, $(M_S - M_R)/M_S = \delta M/M_s \ll 1$, we finally arrive at

$$B \approx \frac{3}{4}\left(\frac{\pi M_S}{b M_5}\right)^{3/2}\frac{\delta M}{M_S}, \tag{38}$$

where $M_5 = (8\pi G_N \ell)^{-1/3}$ is the low energy Planck scale. Fortuitously, the uncertainty in the value of the tidal charge parameter b can be absorbed into our uncertainty in the low energy Planck scale, and so we let $bM_5 \to M_5$.

A. Higgs bubbles on the brane

The Higgs bubble will correspond to a solution of the brane SMS equations with an energy momentum tensor derived from the (Euclidean) scalar field Lagrangian[3]

[3]Note that we have defined the Euclidean Lagrangian to contain $+V$, meaning that the false vacuum solution will have energy momentum $-V g_{\mu\nu}$, but that our 4D Einstein equations will have the conventional sign for the energy momentum, i.e., $G_{\mu\nu} = 8\pi G_N T_{\mu\nu} + \cdots$.

$$\mathcal{L}_m = \frac{1}{2} g^{\mu\nu} \phi_{,\mu} \phi_{,\nu} + V(\phi), \tag{39}$$

where $V(\phi)$ has a metastable false vacuum. The SMS equations for the bubble, assuming the general form (28), are derived in Appendix B and are

$$f\phi'' + f'\phi' + \frac{2}{r} f\phi' + f\delta'\phi' - V_{,\phi} = 0, \tag{40}$$

$$\mu' = 4\pi r^2 \left\{ \frac{1}{2} f\phi'^2 + V - \frac{2\pi G_N}{3} \ell^2 \left(\frac{1}{2} f\phi'^2 - V \right) \times \left(\frac{3}{2} f\phi'^2 + V \right) \right\}, \tag{41}$$

$$\delta' = 4\pi G_N r \phi'^2 \left\{ 1 - \frac{4\pi G_N}{3} \ell^2 \left(\frac{1}{2} f\phi'^2 - V \right) \right\}, \tag{42}$$

where, for comparison with the vacuum case (30), we have defined a "mass" function $\mu(r)$ by

$$f(r) = 1 - \frac{2G_N \mu(r)}{r} - \frac{r_Q^2}{r^2}. \tag{43}$$

These are integrated numerically from the black hole horizon r_h to $r \to \infty$ where ϕ is in the false vacuum. A "shooting" method is used, whereby the value of ϕ at the horizon is varied until a regular solution is found. The remnant mass M_R and the tunneling exponent B are determined in terms of the seed mass M_S, the potential V, and the AdS radius ℓ.

The numerical results contained in this section are based on a Higgs-like potential, assuming that the standard model holds for energy scales up to the low energy Planck mass M_5. The detailed form of the potential is determined by renormalization group methods and depends on low-energy particle masses, with a strong dependence on the Higgs and top quark masses. Of these, the top quark mass is less well known, and for masses in the range 171–174 GeV, Higgs instability sets in at scales from 10^{10}–10^{18} GeV.

The Higgs potential is usually expressed in the form

$$V(\phi) = \frac{1}{4} \lambda_{\rm eff}(\phi) \phi^4 \tag{44}$$

with a running coupling constant $\lambda_{\rm eff}(\phi)$ that becomes negative at some crossover scale Λ_ϕ. Vacuum decay depends on the shape of the potential barrier in the Higgs potential around this instability scale, and in order to explore the likelihood of decay it is useful to use an analytic fit to $\lambda_{\rm eff}$. In [20], we used a two parameter fit to $\lambda_{\rm eff}$, where one of the parameters was closely related to the crossover scale. We found that the dependence of the instanton action on the potential was strongly dependent on this parameter, but very weakly dependent on the second parameter, which was more related to the shape of the potential at low energy. For clarity therefore, here we take a one parameter analytic fit to $\lambda_{\rm eff}$, where the single parameter is the crossover scale Λ_ϕ,

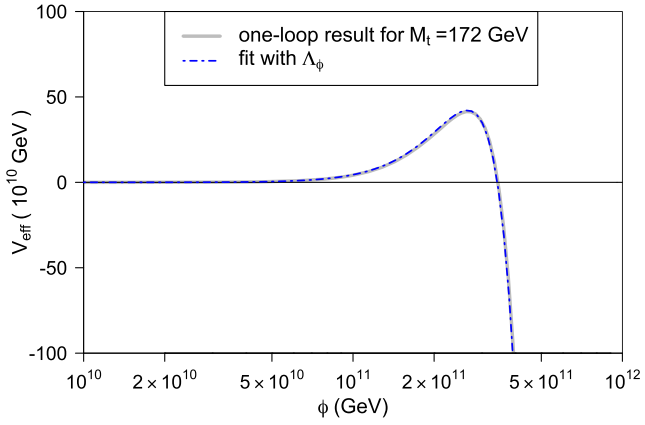

FIG. 4. The Higgs potential calculated numerically at one-loop order for top quark mass $M_t = 172$ GeV and the approximate potential using (45) with values of g and Λ_ϕ chosen for the best fit.

$$\lambda_{\rm eff} = g(\Lambda_\phi) \left\{ \left(\ln \frac{\phi}{M_p} \right)^4 - \left(\ln \frac{\Lambda_\phi}{M_p} \right)^4 \right\}, \tag{45}$$

and $g(\Lambda_\phi)$, chosen to fit the high energy asymptote of $\lambda_{\rm eff}$, varies very little across the range of Λ_ϕ of relevance to the standard model $\lambda_{\rm eff}$. Figure 4 shows a sample of our analytic fit for the Higgs potential to the actual $\lambda_{\rm eff}$ computed for $M_t = 172$ GeV. In four dimensions, we can have a Higgs instability scale very close to the Planck scale; however, with large extra dimensions, new physics could potentially enter at the low-energy Planck scale M_5. Thus to be consistent, we should restrict our parameters to the range $\Lambda_\phi < M_5 < M_p$.

Figure 5 gives profiles for a typical bubble centered on the black hole after tunneling and for the mass term $\mu(r)$ beyond the horizon radius r_h. The field is in the true vacuum at the horizon and approaches the false vacuum as $r \to \infty$ with a characteristic thick wall profile. The bubble radius greatly exceeds the horizon of the black hole.

The change in the mass term is given by $\Delta\mu(r) = \mu(r) - \mu(r_h)$. Near the horizon, $\Delta\mu(r)$ is negative due to the negative potential V in Eq. (41). $\mu(r)$ becomes positive at large r where there is a positive contribution from the kinetic term, and hence ΔM is positive.

B. Branching ratios

The calculation of the vacuum decay rate assumes a stationary background which only makes sense when the decay rate exceeds the Hawking evaporation rate. The brane black hole can radiate in the brane or into the extra dimension, but if we consider a scenario as close as possible

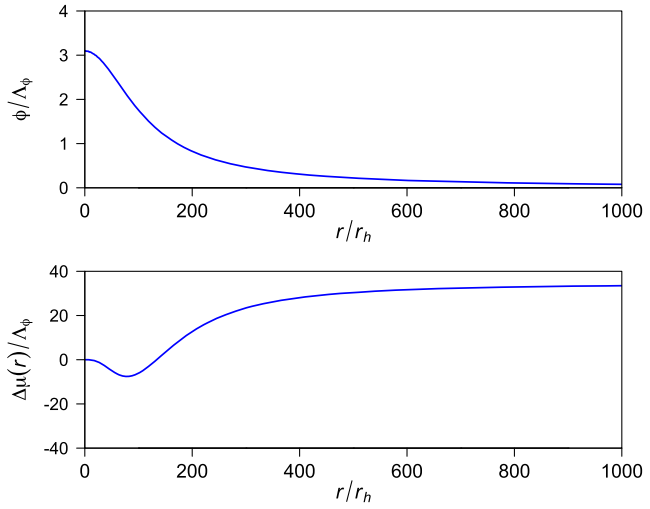

FIG. 5. Profiles for the bubble and the mass term $\mu(r)$ outside the horizon r_h with $M_5 = 10^{15}$ GeV, $\Lambda_\phi = 10^{12}$ GeV, and $r_h = 20000/M_p$. This particular solution has tunneling exponent $B = 4.3$.

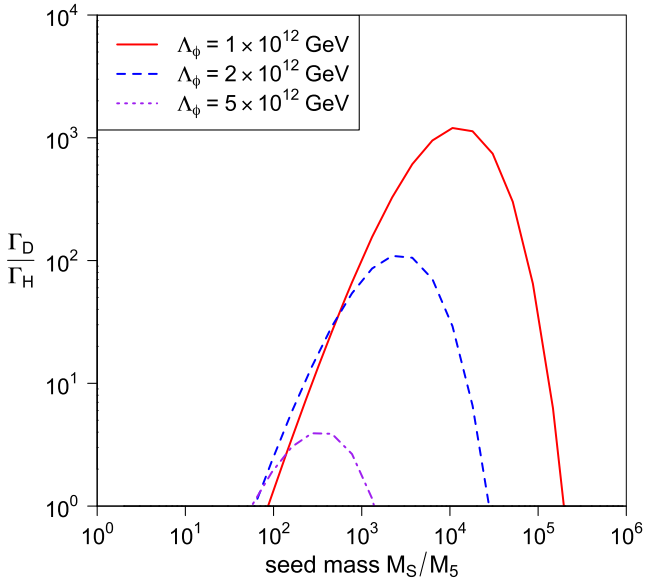

FIG. 6. The branching ratio of the false vacuum nucleation rate to the Hawking evaporation rate as a function of the seed mass for a selection of Higgs models with $M_5 = 10^{15}$ GeV.

to the standard model, then most of the radiation will be in the form of quarks and leptons radiated into the brane, simply because these are the most numerous particles. (For a review of Hawking evaporation rates in higher dimensions see [72].)

Black hole radiation is similar to the radiation from a black body with the same area as the black hole horizon and at the Hawking temperature, but with additional "grey body" factors representing the effects of backscattering of the radiation from the spacetime curvature around the black hole. Following [72], we can express the energy loss rate due to evaporation as $\dot{E}$, where on dimensional grounds (since r_h is the only relevant dimensionful parameter)

$$|\dot{E}| = \gamma r_h^{-2} \tag{46}$$

for some constant γ. The Hawking decay rate of the black hole Γ_H, using (35) to eliminate the radius, is

$$\Gamma_H = \frac{|\dot{E}|}{M_S} = \frac{4\pi\gamma M_5^3}{M_S^2}. \tag{47}$$

The vacuum decay rate is given by

$$\Gamma_D = Ae^{-B}. \tag{48}$$

The prefactor A contains a factor $(B/2\pi)^{1/2}$ from a zero mode and a vacuum polarization term from the other modes, whose characteristic length scale is the bubble radius r_b. We estimate

$$\Gamma_D \approx \left(\frac{B}{2\pi}\right)^{1/2} \frac{1}{r_b} e^{-B}. \tag{49}$$

The branching ratio of the two is

$$\frac{\Gamma_D}{\Gamma_H} \approx \frac{1}{\gamma}\left(\frac{B}{2\pi}\right)^{1/2}\left(\frac{M_S}{M_5}\right)^{3/2}\left(\frac{r_h}{r_b}\right)e^{-B}. \tag{50}$$

Vacuum decay is important when this ratio is larger than one.

In the case of small r_h/ℓ, the five-dimensional black hole has a temperature

$$T \approx \frac{1}{2\pi r_h}, \tag{51}$$

which is double the temperature of a black hole solely in four dimensions. We would therefore expect to have energy flux on the brane roughly $\propto T^4 \sim 16$ times the flux solely in four dimensions. Numerical results actually give a factor of 14.2 for fermion fields, which give the largest contribution to the decay [73]. The energy loss due to a fermion in four dimensions contributes a factor of 7.88×10^{-4} for each degree of freedom to γ, giving a total for 90 standard model fermion degrees of freedom of

$$\gamma \approx 14.2 \times 90 \times 7.88 \times 10^{-4} = 0.10. \tag{52}$$

The branching ratio is plotted in Fig. 6 for $M_5 = 10^{15}$ GeV and the Higgs instability scale around 10^{12} GeV (corresponding to a top quark mass of 172 GeV). Note that the decay rates in this parameter range are larger than M_5^3/M_S^2; i.e., they are extremely fast. The figure shows an example where black holes with masses between 10^{17} GeV and 10^{20} GeV, or 10^{-7}g to 10^{-4}g, would seed rapid Higgs vacuum decay.

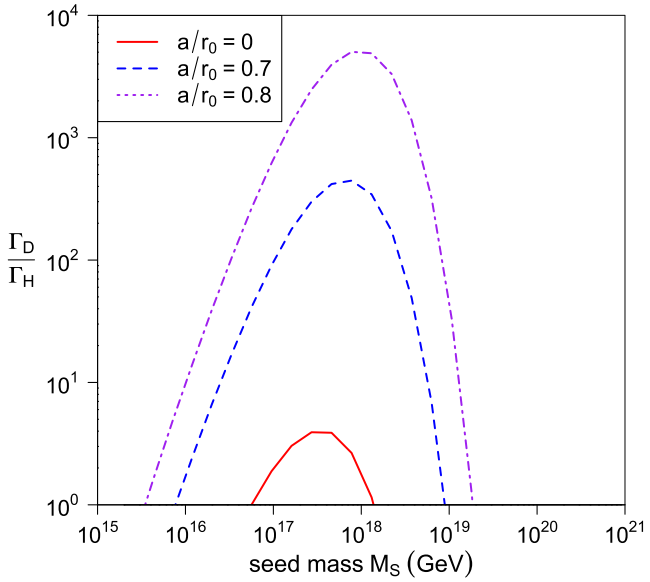

FIG. 7. The branching ratio of the false vacuum nucleation rate to the Hawking evaporation rate as a function of the seed mass for a selection of Higgs models with $M_5 = 10^{15}$ GeV, and $\Lambda_\phi = 5 \times 10^{12}$ GeV.

C. Rotating black holes

Black holes produced by high energy collisions would be likely to be rotating. Rotating tidal black hole solutions [74] can be used as the basis for these black hole seeds. The bubble solutions about these rotating holes will become distorted; however, the profile of the bubble solution (Fig. 5) indicates that much of the variation of the bubble fields occurs at large radii compared to the horizon size of the black hole. This suggests that the distortion will be localized in the small part of the bubble near the black hole, leaving the effective mass δM in the field configuration relatively unaffected. In this case, we can use our earlier result (38) but replacing the horizon area with the area $\mathcal{A}_{\rm MP}$ of a rotating Myers-Perry black hole in flat space [75] when $r_h \ll \ell$,

$$B \approx \frac{\mathcal{A}_{\rm MP}}{4G_5}\frac{3\delta M}{2M_S}. \tag{53}$$

The area depends on two rotation parameters a_1 and a_2, but for a rotation axis aligned to the brane we can take $a_2 = 0$. In this case

$$\mathcal{A}_{\rm MP} = 2\pi^2 r_0^3\left(1 - \frac{a^2}{r_0^2}\right)^{1/2}, \tag{54}$$

where r_0 is the horizon radius of the nonrotating black hole solution,

$$r_0^2 = \frac{8G_5 M_S}{3\pi}. \tag{55}$$

The area is smaller than the nonrotating case. Furthermore, the Hawking temperature is reduced, since

$$T_H = T_0\left(1 - \frac{a^2}{r_0^2}\right)^{1/2}. \tag{56}$$

The numerical results for vacuum decay are shown in Fig. 7. The vacuum decay rate Ae^{-B} with rotating seeds is larger than with nonrotating seeds due to the reduced area.

V. CONCLUSIONS

In this paper we have explored the impact of large extra dimensions on black hole seeded vacuum decay. We used the Randall-Sundrum setup as a concrete example for warped extra dimensions, and we numerically computed the Higgs profile on the brane for vacuum decay assuming a *tidal Ansatz* for the Weyl tensor on the brane. Although the solution for a brane black hole is not known analytically, we were nonetheless able to construct an argument that the action for tunneling would still be the difference in areas of the black hole horizons. In order to estimate these areas, we focused on small brane black holes (expected to be the most relevant for vacuum decay) and used qualitative features of the numerical solutions to argue the black hole area would be very well approximated by the hyperspherical result $2\pi^2 r_h^3$. We then used the tidal model for a brane black hole (in keeping with the tidal Ansatz for the Weyl tensor), expanded for small masses, to relate the 4D brane mass of the black hole, the $1/r$ falloff of the Newtonian potential, to the horizon radius. This then allowed us to compute the amplitude for tunneling.

Since a black hole can also radiate, we then have to consider whether the evaporation rate is so fast that the tunneling amplitude is irrelevant, or whether the tunneling probability becomes so high for small black holes (as was the case for purely four-dimensional black holes [20]) that the black hole always initiates decay. We therefore estimated the net evaporation rate by taking the integrated flux from [73], which is dominated by the fermion radiation, and summing up the effect from the standard model particles. The branching ratio plot of Fig. 6 demonstrates that, just as in 4D, small black holes in higher dimensions are overwhelmingly likely to initiate vacuum decay once they have radiated away sufficient mass to enter this danger range. As with pure 4D, any small black hole, formed either in the early universe or in a high energy cosmic ray collision, will radiate, lose mass, and then become sufficiently light that it seeds decay with a rate of order $10^{3-5}T_5$.[4] What is interesting here is that what we mean by *small* is now very different from the pure 4D case.

With large extra dimensional scenarios, we generate a high 4D Planck scale geometrically, having a renormalization of the Newton constant coming from the "volume" of the internal dimensions. Thus, in 4D, where the typical black hole seeding vacuum decay for the Higgs was in the range

[4]Here, $T_5 = (c^3/8\pi G_5\hbar)^{1/3}$ is the 5D Planck time.

10^5–$10^9 M_p \simeq 1\text{g} - 10$ tonnes, these black holes could only be primordial in origin, having far too high a mass to be produced in a particle collision. Here, however, our Planck mass can be much lower, so $10^5 M_5$ can potentially be sufficiently low that the black hole could be produced in a cosmic ray collision. For example, the highest energy cosmic ray collisions [76–78] observed have an energy in excess of 10^{11} GeV. Hut and Rees [79] have shown that there are at least 10^5 collisions with center of mass energy exceeding 10^{11} GeV in our past light cone. Thus, provided the higher-dimensional Planck scales were below $M_5 \lesssim 10^9$ GeV, black holes could be formed in a cosmic ray collision that would be sufficiently light to catalyze vacuum decay.

In the context of the Higgs field, the standard model potential is only valid at best for energy scales below the scale of new physics, M_5; therefore the instability scale should satisfy $\Lambda_\phi < M_5$. The lowest possible value for the instability scale consistent with experimental limits on the top quark mass is around 10^8 GeV, and thus we cannot use our standard model Higgs decay results unless $M_5 \gg 10^8$ GeV, well outside the range probed by the LHC.

As an example, consider an instability scale $\Lambda_\phi \sim 10^8$ GeV and a Planck scale $M_5 \sim 10^9$ GeV; then black holes of mass $M_S \sim 10^{11}$ GeV could cause Higgs vacuum decay. These values are below those for which we were able to obtain numerical results, but we can make a rough approximation by taking the exponent for vacuum decay B from (38), and the mass of the instanton $\delta M \sim \Lambda_\phi$. For these values we estimate $B = O(1)$ and rapid Higgs decay would take place.

While this is a rather rough argument, the basic intuition that the branching ratio will be enhanced by both the larger decay rate and the reduced Hawking evaporation rate is likely to be correct. In other words, if the existence of large extra dimensions does not destroy the vacuum metastability of the standard model Higgs, then ultrahigh energy particle collisions risk producing black hole seeds that will catalyze the decay of the vacuum.

ACKNOWLEDGMENTS

We are grateful for the hospitality of the Perimeter Institute, where part of this research was undertaken. This work was supported in part by the Leverhulme grant *Challenging the Standard Model with Black Holes* and in part by STFC consolidated Grant No. ST/P000371/1. L. C. acknowledges financial support from CONACyT, R. G. is supported in part by the Perimeter Institute for Theoretical Physics, and K. M. is supported by an STFC studentship. Research at Perimeter Institute is supported by the Government of Canada through the Department of Innovation, Science and Economic Development Canada and by the Province of Ontario through the Ministry of Research, Innovation and Science.

APPENDIX A: CANONICAL DECOMPOSITION

In this appendix we review and extend the ideas given in [65] that provide a canonical decomposition of a manifold (in our case a Euclidean one) by a foliation of hypersurfaces Σ_τ to recast the gravitational action in its Hamiltonian version.

The gravitational equations on a manifold $\mathcal{M}$ with boundary $\partial\mathcal{M}$ are obtained by the extremization of the usual Einstein-Hilbert action plus a Gibbons-Hawking surface term:

$$I = -\frac{1}{16\pi G_5}\int_{\mathcal{M}} (R_5 - 2\Lambda_5)\sqrt{g_5} + \int_{\mathcal{B}} \mathcal{L}_m(g,\phi)\sqrt{g_4} + \frac{1}{8\pi G_5}\int_{\partial\mathcal{M}} \sqrt{h}K, \tag{A1}$$

where $\mathcal{L}_m$ is the matter Lagrangian, $h_{ab} = g_{ab} - n_a n_b$ is the induced metric, and $K = g^{ab}K_{ab} = g^{ab}h_a{}^c h_b{}^d \nabla_c n_d$ is the trace of the extrinsic curvature of the boundary $\partial\mathcal{M}$ with normal vector n_a pointing *in* to $\mathcal{M}$ (Fig. 8).

To simplify this action we make a foliation of the spacetime $\mathcal{M}$ by codimension one time slices Σ_τ, labeled by a periodic Euclidean time function τ which runs from $\tau = 0$ to $\tau = \beta$. The induced metric on the time slices is written as

$$\mathfrak{h}_{ab} = g_{ab} - u_a u_b, \tag{A2}$$

where u^a is a unit normal vector to the slice Σ_τ. In general, $\partial/\partial\tau$ and u^a will not be aligned, but we can decompose $\partial/\partial\tau$ into components along the normal and tangential directions,

$$\left(\frac{\partial}{\partial\tau}\right)^a = N u^a + N^a. \tag{A3}$$

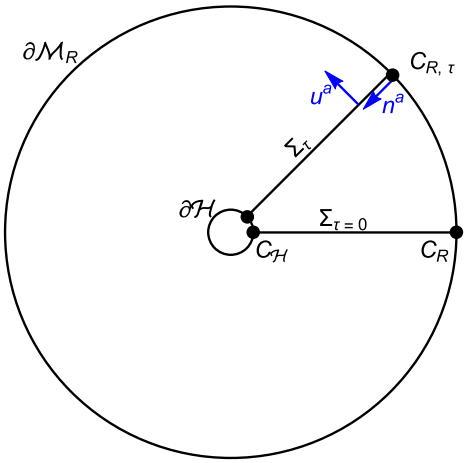

FIG. 8. The foliation of the Euclidean $\{\tau, r\}$ section of the brane black hole. The normals u^a and n^a of, respectively, the foliation Σ_τ and manifold boundaries are shown, together with the codimension two surfaces $C_{R,\tau}$ that are regarded as a codimension one submanifold of the Σ_τ surfaces.

The *lapse function*, N, measures the rate of flow of proper time with respect to the coordinate time τ as one moves through the family of hypersurfaces. We construct the time slices Σ_τ to meet the boundary $\partial\mathcal{M}$ orthogonally for convenience. In the case of the region outside the horizon for $I_R^{\rm ext}$ (15), the boundary $\partial\mathcal{M}$ is composed of two surfaces of constant radius, $\Sigma_\mathcal{H}$ near the horizon, and Σ_R at large radius.

We use the Gauss identity to relate the Riemann tensor of g_{ab} in five dimensions to the Riemann tensor of $\mathfrak{h}_{ab}$ in four, and the extrinsic curvatures of the constant time slices $\mathcal{K}_{ab} = \mathfrak{h}^c{}_a\mathfrak{h}^d{}_b\nabla_c u_d$, as

$$R_4{}^a{}_{bcd} = \mathfrak{h}^a{}_{a'}\mathfrak{h}_b{}^{b'}\mathfrak{h}_c{}^{c'}\mathfrak{h}_d{}^{d'}R_5{}^{a'}{}_{b'c'd'} + \mathcal{K}^a{}_c\mathcal{K}_{db} - \mathcal{K}^a{}_d K_{cb}. \tag{A4}$$

Notice this $\mathcal{K}$ is distinct from the extrinsic curvature of Σ_R in (A1). Contracting (A4) gives

$$R_5 = R_4 + 2R_{5ab}u^a u^b - (\mathcal{K}^2 - \mathcal{K}^{ab}\mathcal{K}_{ab}), \tag{A5}$$

and we obtain a relation between the second term of this expression and the extrinsic curvature by commuting covariant derivatives of the normal vector

$$R_{5ab}u^a u^b = 2u^b\nabla_{[c}\nabla_{b]}u^c = \mathcal{K}^2 - \mathcal{K}^{ab}\mathcal{K}_{ab} - \nabla_a(u^a\nabla_c u^c) + \nabla_c(u^a\nabla_a u^c). \tag{A6}$$

Combining these two expressions leads to the identity

$$R_5 = R_4 - (\mathcal{K}^{ab}\mathcal{K}_{ab} - \mathcal{K}^2) - 2[\nabla_a(u^a\nabla_c u^c) - \nabla_c(u^a\nabla_a u^c)], \tag{A7}$$

which forms the basis of all canonical decompositions of the Einstein-Hilbert action.

When substituted in (A1), the last two terms of (A7) are reduced to boundary contributions on $\partial\mathcal{M}$. The first of these vanishes due to orthogonality of $\partial\mathcal{M}_R$ and Σ_τ. The second combines with $\int_{\partial\mathcal{M}} K$ from the original action and gives on $\partial\mathcal{M}_R$ (with a similar expression for $\partial\mathcal{H}$)

$$\begin{aligned}&\frac{1}{8\pi G_5}\int_{\partial\mathcal{M}_R} d^4x\sqrt{h}(\nabla_a n^a + n_b u^a\nabla_a u^b)\\ &= \frac{1}{8\pi G_5}\int_{\partial\mathcal{M}_R} d^4x\sqrt{h}(g^{ab} - u^a u^b)\nabla_a n_b\\ &= \frac{1}{8\pi G_5}\int_{\partial\mathcal{M}_R} d^4x\sqrt{h}\mathfrak{h}^{ab}\nabla_a n_b,\end{aligned} \tag{A8}$$

but this four-dimensional integral can be viewed as an integral over τ of a three-dimensional integrand that is precisely the three-dimensional extrinsic curvature ${}^3K$ of a family of surfaces $C_R(\tau) = \partial\mathcal{M}_R \cap \Sigma_\tau$ living in the boundary $\partial\mathcal{M}_R$. A similar term is obtained for the $\partial\mathcal{H}$ surface near the horizon; however, for the black hole metrics, it turns out that ${}^3K \to 0$ as $r \to r_h$, and so this term does not contribute to the action.

Noticing that $\sqrt{g} = N\sqrt{\mathfrak{h}}$, and introducing a metric ${}^3\mathfrak{h}$ on C_R, we can divide the spacetime integral into space and time, to express the action (A1) as

$$I = -\int N d\tau\left\{\frac{1}{16\pi G_5}\int_{\Sigma_\tau}\sqrt{\mathfrak{h}}[R_4 - (\mathcal{K}^{ab}\mathcal{K}_{ab} - \mathcal{K}^2) - 2\Lambda_5 - 16\pi G_5\mathcal{L}_m] - \frac{1}{8\pi G_5}\int_{C_R}\sqrt{{}^3\mathfrak{h}}{}^3K - \frac{1}{8\pi G_5}\int_{C_\mathcal{H}}\sqrt{{}^3\mathfrak{h}}{}^3K\right\}. \tag{A9}$$

Furthermore, we can see how the extrinsic curvature is related to the Lie derivative of the intrinsic metric with respect to τ via (A3),

$$\begin{aligned}\mathcal{K}_{ab} &= \frac{1}{2}\pounds_u\mathfrak{h}_{ab} = \frac{1}{2N}(\pounds_\tau\mathfrak{h}_{ab} - \pounds_N\mathfrak{h}_{ab})\\ &= \frac{1}{2N}(\dot{\mathfrak{h}}_{ab} - 2D_{(a}N_{b)}),\end{aligned} \tag{A10}$$

where $\dot{\mathfrak{h}}_{ab} = \mathfrak{h}^c_a\mathfrak{h}^d_b\pounds_\tau\mathfrak{h}_{cd}$ and D_a is the derivative associated with $\mathfrak{h}_{ab}$.

To obtain the Hamiltonian form of I we define the canonical momentum π^{ab} conjugate to the intrinsic metric as

$$\pi^{ab} \equiv \frac{\delta I}{\delta\dot{\mathfrak{h}}_{ab}} = \sqrt{\mathfrak{h}}(\mathcal{K}^{ab} - \mathcal{K}\mathfrak{h}^{ab}). \tag{A11}$$

This allows us to recast (A9) in terms of the canonical momentum

$$I = -\int_0^\beta N d\tau\left\{\frac{1}{16\pi G_5}\int_{\Sigma_\tau}\sqrt{\mathfrak{h}}\left[R_4 - \frac{1}{\mathfrak{h}}\left(\pi^{ab}\pi_{ab} - \frac{1}{3}\pi^2\right) - 2\Lambda_5 - 16\pi G_5\mathcal{L}_m\right] - \frac{1}{8\pi G_5}\int_{C_R}\sqrt{{}^3\mathfrak{h}}{}^3K - \frac{1}{8\pi G_5}\int_{C_\mathcal{H}}\sqrt{{}^3\mathfrak{h}}{}^3K\right\}. \tag{A12}$$

Now we are ready to perform a Legendre transformation of the Lagrangian, using (A10) and (A11) to obtain the Hamiltonian formulation,

$$I = \frac{1}{8\pi G_5}\int_0^\beta d\tau\left\{\frac{1}{2}\int_{\Sigma_\tau}\sqrt{\mathfrak{h}}(\pi^{ab}\dot{\mathfrak{h}}_{ab} - N\mathcal{H} - N^a\mathcal{H}_a) + \int_{C_R}\sqrt{{}^3\mathfrak{h}}(N^3K + N^a\pi_{ab}n^b) + \int_{C_\mathcal{H}}\sqrt{{}^3\mathfrak{h}}(N^3K + N^a\pi_{ab}n^b)\right\}, \tag{A13}$$

with the *Hamiltonian constraint* function $\mathcal{H}$ and the *momentum constraint* function $\mathcal{H}^a$ given by

$$\mathcal{H}^a = -2D_b\left(\frac{1}{\sqrt{\mathfrak{h}}}\pi^{ab}\right),$$
$$\mathcal{H} = R_4 - 2\Lambda_5 + \frac{1}{\mathfrak{h}}\left(\pi^{ab}\pi_{ab} - \frac{1}{3}\pi^2\right) - 16\pi G_5\mathcal{L}_m. \tag{A14}$$

Finally, for a static spacetime we have $\dot{\mathfrak{h}}_{ab} = 0$ and in the nonrotating case $N^a = 0$. The metric is a solution to the field equations, so that in particular we have the constraint equations $\mathcal{H} = \mathcal{H}^a = 0$. The only nonvanishing part of the action are the two boundary terms ${}^3K$,

$$I = \frac{1}{8\pi G_5}\int_0^\beta d\tau\left(\int_{C_R} {}^3K\sqrt{h} + \int_{C_\mathcal{H}} {}^3K\sqrt{h}\right). \tag{A15}$$

For our black hole solutions, this diverges in the limit $R \to 0$. However, the matter contributions to the black hole instanton solutions die off exponentially at large radii, so that the boundary terms cancel when we calculate the difference in actions between the instanton solutions and the false vacuum solutions with the same mass and periodicity β.

APPENDIX B: BRANE EQUATIONS FOR THE INSTANTON BUBBLE

Following the work done in [52,53] we briefly review the derivation of the equations (40)–(42), which describe the dynamics of the bubble-brane system analyzed in Sec. IV.

The Einstein equations for a five-dimensional RS brane-world can be written as

$${}^{(5)}G_{ab} = -\Lambda_5 g_{ab} + 8\pi G_5\delta(z)(-\sigma h_{ab} + T_{ab}), \tag{B1}$$

where z is a coordinate defined by taking the proper distance from the brane into the bulk, $G_5 = G_N\ell$, and the cosmological constant of the bulk $\Lambda_5 = -6/\ell^2$ is given in terms of the AdS_5 radius ℓ. Notice that we use latin indices for the bulk spacetime, whereas greek indices will be reserved for objects living on the brane. The brane is located at $z = 0$ and has an induced metric h_{ab}, defined by

$$h_{ab} = g_{ab} - n_a n_b, \tag{B2}$$

where n^a is a unit vector in the z direction. The energy momentum tensor of the brane carries the effect of the tension σ and has a contribution T_{ab}, coming from the fields living in the brane.

The Israel junction conditions for the brane allow us to write down a set of four-dimensional Einstein equations (see [52]),

$$G_{\mu\nu} = 8\pi G_N\tilde{T}_{\mu\nu} - \mathcal{E}_{\mu\nu} - \Lambda_{\text{eff}}h_{\mu\nu}, \tag{B3}$$

where Λ_{eff} is an effective four-dimensional cosmological constant on the brane,

$$\Lambda_{\text{eff}} = -\frac{3}{\ell^2} + \frac{(4\pi G_5\sigma)^2}{3}, \tag{B4}$$

and $\mathcal{E}_{\mu\nu}$ is the projection of the five-dimensional Weyl tensor onto the brane,

$$\mathcal{E}_{\mu\nu} = {}^{(5)}C^\alpha{}_{\beta\rho\sigma}n_\alpha n^\rho h_\mu{}^\beta h_\nu{}^\sigma, \tag{B5}$$

carrying information about the extra dimensional geometry to the brane. Because of the properties of the Riemann tensor, $\mathcal{E}_{\mu\nu}$ is traceless and divergence-free. In the critical RS brane that will be our false vacuum, the tension of the brane is tuned so as to set Λ_{eff} to zero, i.e.,

$$\sigma = \frac{3}{4\pi G_5\ell}. \tag{B6}$$

Finally, the effective energy momentum tensor, $\tilde{T}_{\mu\nu} = T_{\mu\nu} + \pi_{\mu\nu}$, consists of the standard energy momentum tensor, together with second order terms

$$\pi_{\mu\nu} = \frac{1}{\sigma}\left(-\frac{3}{2}T_{\mu\alpha}T^\alpha_\nu + \frac{1}{2}TT_{\mu\nu} + \frac{3}{4}h_{\mu\nu}T_{\alpha\beta}T^{\alpha\beta} - \frac{1}{4}h_{\mu\nu}T^2\right). \tag{B7}$$

As discussed in Sec. IV, we consider static, spherically symmetric solutions on the brane, with metric (28), and make the tidal Ansatz for the Weyl tensor,

$$\mathcal{E}_{\mu\nu}dx^\mu dx^\nu = \mathcal{U}(r)(fe^{2\delta}d\tau^2 + f^{-1}dr^2 - r^2d\Omega_{II}^2), \tag{B8}$$

where the conservation equation gives

$$\mathcal{U}(r) = -\frac{r_Q^2}{r^4}. \tag{B9}$$

The metric functions $f(r)$ and $\delta(r)$ are determined by the effective Einstein equations (B3). Following [20], we define a "mass function" $\mu(r)$ by

$$f = 1 - \frac{2G_N\mu(r)}{r} - \frac{r_Q^2}{r^2}, \tag{B10}$$

where we have explicitly factored out the tidal term r_Q^2/r^2. The relevant components of the Einstein tensor are

$$G^t{}_t = -\frac{2G_N\mu'}{r^2} + \frac{r_Q^2}{r^4}, \qquad G^r{}_r - G^t{}_t = \frac{2f}{r}\delta'. \tag{B11}$$

For the instanton scalar profile with potential $V(\phi)$, the energy-momentum tensor for the scalar field is

$$T_{\mu\nu} = \phi'^2\delta^r_\mu\delta^r_\nu - h_{\mu\nu}\left(\frac{1}{2}f\phi'^2 + V\right), \tag{B12}$$

and thus inputting the form of f, we see that the tidal contribution is canceled by the tidal tensor, and we finally obtain the equations of motion (40)–(42) used in the numerical integration:

$$
\begin{aligned}
0 &= f\phi'' + \frac{2}{r}f\phi' + \delta' f\phi' + f'\phi' - \frac{\partial V}{\partial \phi}, \\
\mu'(r) &= 4\pi r^2\left[\frac{1}{2}f\phi'^2 + V - \frac{2\pi G_N}{3}\ell^2\left(\frac{1}{2}f\phi'^2 - V\right)\left(\frac{3}{2}f\phi'^2 + V\right)\right], \\
\delta' &= 4\pi G_N r\phi'^2\left[1 - \frac{4\pi G_N}{3}\ell^2\left(\frac{1}{2}f\phi'^2 - V\right)\right].
\end{aligned} \tag{B13}
$$

[1] G. Aad *et al.* (ATLAS Collaboration), Combined search for the Standard Model Higgs boson using up to 4.9 fb^{-1} of pp collision data at $\sqrt{s} = 7$ TeV with the ATLAS detector at the LHC, Phys. Lett. B **710**, 49 (2012).

[2] S. Chatrchyan *et al.* (CMS Collaboration), Combined results of searches for the standard model Higgs boson in pp collisions at $\sqrt{s} = 7$ TeV, Phys. Lett. B **710**, 26 (2012).

[3] G. Degrassi, S. Di Vita, J. Elias-Miro, J. R. Espinosa, G. F. Giudice, G. Isidori, and A. Strumia, Higgs mass and vacuum stability in the Standard Model at NNLO, J. High Energy Phys. 08 (2012) 098.

[4] A. Gorsky, A. Mironov, A. Morozov, and T. N. Tomaras, Is the Standard Model saved asymptotically by conformal symmetry?, Zh. Eksp. Teor. Fiz. **147**, 399 (2015) [J. Exp. Theor. Phys. **120**, 344 (2015)].

[5] F. Bezrukov and M. Shaposhnikov, Why should we care about the top quark Yukawa coupling?, Zh. Eksp. Teor. Fiz. **147**, 389 (2015).

[6] J. Ellis, Discrete glimpses of the physics landscape after the Higgs discovery, J. Phys. Conf. Ser. **631**, 012001 (2015).

[7] K. Blum, R. T. D'Agnolo, and J. Fan, Vacuum stability bounds on Higgs coupling deviations, J. High Energy Phys. 03 (2015) 166.

[8] I. V. Krive and A. D. Linde, On the vacuum stability problem in gauge theories, Nucl. Phys. **B432**, 265 (1976).

[9] M. S. Turner and F. Wilczek, Is our vacuum metastable, Nature (London) **298**, 633 (1982).

[10] M. Sher, Electroweak Higgs potentials and vacuum stability, Phys. Rep. **179**, 273 (1989).

[11] G. Isidori, G. Ridolfi, and A. Strumia, On the metastability of the standard model vacuum, Nucl. Phys. **B609**, 387 (2001).

[12] J. Elias-Miro, J. R. Espinosa, G. F. Giudice, G. Isidori, A. Riotto, and A. Strumia, Higgs mass implications on the stability of the electroweak vacuum, Phys. Lett. B **709**, 222 (2012).

[13] S. Coleman, Fate of the false vacuum: Semiclassical theory, Phys. Rev. D **15**, 2929 (1977).

[14] C. G. Callan and S. Coleman, Fate of the false vacuum II: First quantum corrections, Phys. Rev. D **16**, 1762 (1977).

[15] S. Coleman and F. De Luccia, Gravitational effects on and of vacuum decay, Phys. Rev. D **21**, 3305 (1980).

[16] I. Y. Kobzarev, L. B. Okun, and M. B. Voloshin, Bubbles in metastable vacuum, Yad. Fiz. **20**, 1229 (1974) [Sov. J. Nucl. Phys. **20**, 644 (1975)].

[17] R. Gregory, I. G. Moss, and B. Withers, Black holes as bubble nucleation sites, J. High Energy Phys. 03 (2014) 081.

[18] P. Burda, R. Gregory, and I. Moss, Gravity and the Stability of the Higgs Vacuum, Phys. Rev. Lett. **115**, 071303 (2015).

[19] P. Burda, R. Gregory, and I. Moss, Vacuum metastability with black holes, J. High Energy Phys. 08 (2015) 114.

[20] P. Burda, R. Gregory, and I. Moss, The fate of the Higgs vacuum, J. High Energy Phys. 06 (2016) 025.

[21] R. Gregory and I. G. Moss, The Fate of the Higgs Vacuum, Proc. Sci., ICHEP2016 (**2016**) 344 [arXiv:1611.04935].

[22] N. Tetradis, Black holes and Higgs stability, J. Cosmol. Astropart. Phys. 09 (2016) 036.

[23] P. Chen, G. DomËnech, M. Sasaki, and D. h. Yeom, Thermal activation of thin-shells in anti-de Sitter black hole spacetime, J. High Energy Phys. 07 (2017) 134.

[24] D. Gorbunov, D. Levkov, and A. Panin, Fatal youth of the Universe: Black hole threat for the electroweak vacuum during preheating, J. Cosmol. Astropart. Phys. 10 (2017) 016.

[25] K. Mukaida and M. Yamada, False vacuum decay catalyzed by black holes, Phys. Rev. D **96**, 103514 (2017).

[26] N. Arkani-Hamed, S. Dimopoulos, and G. R. Dvali, The Hierarchy problem and new dimensions at a millimeter, Phys. Lett. B **429**, 263 (1998).

[27] I. Antoniadis, N. Arkani-Hamed, S. Dimopoulos, and G. R. Dvali, New dimensions at a millimeter to a Fermi and superstrings at a TeV, Phys. Lett. B **436**, 257 (1998).

[28] L. Randall and R. Sundrum, A Large Mass Hierarchy from a Small Extra Dimension, Phys. Rev. Lett. **83**, 3370 (1999).

[29] L. Randall and R. Sundrum, An Alternative to Compactification, Phys. Rev. Lett. **83**, 4690 (1999).

[30] S. Dimopoulos and G. L. Landsberg, Black Holes at the LHC, Phys. Rev. Lett. **87**, 161602 (2001).

[31] S. B. Giddings and S. D. Thomas, High-energy colliders as black hole factories: The end of short distance physics, Phys. Rev. D **65**, 056010 (2002).

[32] G. L. Landsberg, Black holes at future colliders and in cosmic rays, Eur. Phys. J. C **33**, S927 (2004).

[33] C. M. Harris, M. J. Palmer, M. A. Parker, P. Richardson, A. Sabetfakhri, and B. R. Webber, Exploring higher dimensional black holes at the Large Hadron Collider, J. High Energy Phys. 05 (2005) 053.

[34] S. C. Park, Black holes and the LHC: A Review, Prog. Part. Nucl. Phys. **67**, 617 (2012).

[35] W. Israel, Singular hypersurfaces and thin shells in general relativity, Nuovo Cimento Soc. Ital. Phys. **B44**, 1 (1966).

[36] R. P. Geroch and J. H. Traschen, Strings and other distributional sources in general relativity, Phys. Rev. D **36**, 1017 (1987).

[37] H. A. Chamblin and H. S. Reall, Dynamic dilatonic domain walls, Nucl. Phys. **B562**, 133 (1999).
[38] N. Kaloper, Bent domain walls as braneworlds, Phys. Rev. D **60**, 123506 (1999).
[39] P. Kraus, Dynamics of anti-de Sitter domain walls, J. High Energy Phys. 12 (1999) 011.
[40] P. Binetruy, C. Deffayet, and D. Langlois, Non-conventional cosmology from a brane-universe, Nucl. Phys. **B565**, 269 (2000).
[41] P. Bowcock, C. Charmousis, and R. Gregory, General brane cosmologies and their global spacetime structure, Classical Quantum Gravity **17**, 4745 (2000).
[42] A. Karch and L. Randall, Open and closed string interpretation of SUSY CFT's on branes with boundaries, J. High Energy Phys. 06 (2001) 063.
[43] R. Gregory, Braneworld black holes, Lect. Notes Phys. **769**, 259 (2009).
[44] P. Kanti, Brane-World Black Holes, J. Phys. Conf. Ser. **189**, 012020 (2009).
[45] A. Chamblin, S. W. Hawking, and H. S. Reall, Brane-world black holes, Phys. Rev. D **61**, 065007 (2000).
[46] R. Gregory, Black string instabilities in anti-de Sitter space, Classical Quantum Gravity **17**, L125 (2000).
[47] R. Gregory and R. Laflamme, Black Strings and p-Branes are Unstable, Phys. Rev. Lett. **70**, 2837 (1993).
[48] R. Emparan, G. T. Horowitz, and R. C. Myers, Exact description of black holes on branes, J. High Energy Phys. 01 (2000) 007.
[49] R. Emparan, G. T. Horowitz, and R. C. Myers, Exact description of black holes on branes. II: Comparison with BTZ black holes and black strings, J. High Energy Phys. 01 (2000) 021.
[50] W. Kinnersley and M. Walker, Uniformly accelerating charged mass in general relativity, Phys. Rev. D **2**, 1359 (1970).
[51] J. F. Plebanski and M. Demianski, Rotating, charged, and uniformly accelerating mass in general relativity, Ann. Phys. (N.Y.) **98**, 98 (1976).
[52] T. Shiromizu, K. i. Maeda, and M. Sasaki, The Einstein equation on the 3-brane world, Phys. Rev. D **62**, 024012 (2000).
[53] N. Dadhich, R. Maartens, P. Papadopoulos, and V. Rezania, Black Holes on the Brane, Phys. Lett. B **487**, 1 (2000).
[54] C. Galfard, C. Germani, and A. Ishibashi, Asymptotically AdS brane black holes, Phys. Rev. D **73**, 064014 (2006).
[55] S. Creek, R. Gregory, P. Kanti, and B. Mistry, Braneworld stars and black holes, Classical Quantum Gravity **23**, 6633 (2006).
[56] D. C. Dai and D. Stojkovic, Analytic solution for a static black hole in RSII model, Phys. Lett. B **704**, 354 (2011).
[57] P. Kanti, N. Pappas, and K. Zuleta, On the localization of four-dimensional brane-world black holes, Classical Quantum Gravity **30**, 235017 (2013).
[58] T. Wiseman, Relativistic stars in Randall-Sundrum gravity, Phys. Rev. D **65**, 124007 (2002).
[59] H. Kudoh, T. Tanaka, and T. Nakamura, Small localized black holes in brane world: Formulation and numerical method, Phys. Rev. D **68**, 024035 (2003).
[60] P. Figueras and T. Wiseman, Gravity and Large Black Holes in Randall-Sundrum II Braneworlds, Phys. Rev. Lett. **107**, 081101 (2011).
[61] D. Wang and M. W. Choptuik, Black Hole Formation in Randall-Sundrum II Braneworlds, Phys. Rev. Lett. **117**, 011102 (2016).
[62] R. Gregory and A. Padilla, Brane world instantons, Classical Quantum Gravity **19**, 279 (2002).
[63] H. Kudoh and Y. Kurita, Thermodynamics of four-dimensional black objects in the warped compactification, Phys. Rev. D **70**, 084029 (2004).
[64] C. M. Harris, P. Richardson, and B. R. Webber, CHARYBDIS: A black hole event generator, J. High Energy Phys. 08 (2003) 033.
[65] S. W. Hawking and G. T. Horowitz, The gravitational Hamiltonian, action, entropy and surface terms, Classical Quantum Gravity **13**, 1487 (1996).
[66] J. Garriga and T. Tanaka, Gravity in the Brane World, Phys. Rev. Lett. **84**, 2778 (2000).
[67] V. Balasubramanian and P. Kraus, A stress tensor for Anti-de Sitter gravity, Commun. Math. Phys. **208**, 413 (1999).
[68] R. Emparan, C. V. Johnson, and R. C. Myers, Surface terms as counterterms in the AdS/CFT correspondence, Phys. Rev. D **60**, 104001 (1999).
[69] R. Maartens, Cosmological dynamics on the brane, Phys. Rev. D **62**, 084023 (2000).
[70] R. Gregory, R. Whisker, K. Beckwith, and C. Done, Observing braneworld black holes, J. Cosmol. Astropart. Phys. 10 (2004) 013.
[71] R. Maartens and K. Koyama, Brane-world gravity, Living Rev. Relativity **13**, 5 (2010).
[72] P. Kanti and E. Winstanley, Hawking radiation from higher-dimensional black holes, Fund. Theor. Phys. **178**, 229 (2015).
[73] C. M. Harris and P. Kanti, Hawking radiation from a $(4+n)$-dimensional black hole: Exact results for the Schwarzschild phase, J. High Energy Phys. 10 (2003) 014.
[74] A. N. Aliev and A. E. Gumrukcuoglu, Charged rotating black holes on a 3-brane, Phys. Rev. D **71**, 104027 (2005).
[75] R. C. Myers and M. J. Perry, Black holes in higher dimensional space-times, Ann. Phys. (N.Y.) **172**, 304 (1986).
[76] J. Linsley, Evidence for a Primary Cosmic-Ray Particle with Energy 10^{20} eV, Phys. Rev. Lett. **10**, 146 (1963).
[77] M. Nagano and A. A. Watson, Observations and implications of the ultrahigh-energy cosmic rays, Rev. Mod. Phys. **72**, 689 (2000).
[78] A. Aab *et al.* (Pierre Auger Collaboration), Measurement of the cosmic ray spectrum above 4×10^{18} eV using inclined events detected with the Pierre Auger Observatory, J. Cosmol. Astropart. Phys. 08 (2015) 049.
[79] P. Hut and M. J. Rees, How stable is our vacuum?, Nature (London) **302**, 508 (1983).